Analysis of laser-proton acceleration experiments for development of empirical scaling laws

M. Zimmer,[1,*] S. Scheuren,[1] T. Ebert,[1] G. Schaumann,[1] B. Schmitz,[2] J. Hornung,[3,4,5] V. Bagnoud,[1,3] C. Rödel,[1] and M. Roth[1]

[1]*Institute of Nuclear Physics, Technical University of Darmstadt, Schlossgartenstr. 9, 64289 Darmstadt, Germany*
[2]*Institute for Accelerator Science and Electromagnetic Fields, Technical University of Darmstadt, Schlossgartenstr. 8, 64289 Darmstadt, Germany*
[3]*GSI Helmholtz Centre for Heavy Ion Research, Planckstr. 1, 64291 Darmstadt, Germany*
[4]*Friedrich-Schiller-Universität Jena, Fürstengraben 1, 07743 Jena, Germany*
[5]*Helmholtz-Institut Jena, Fröbelstieg 3, 07743 Jena, Germany*

(Received 8 February 2021; accepted 13 September 2021; published 25 October 2021; corrected 2 November 2021)

Numerous experiments on laser-driven proton acceleration in the MeV range have been performed with a large variety of laser parameters since its discovery around the year 2000. Both experiments and simulations have revealed that protons are accelerated up to a maximum cut-off energy during this process. Several attempts have been made to find a universal model for laser proton acceleration in the target normal sheath acceleration regime. While these models can qualitatively explain most experimental findings, they can hardly be used as predictive models, for example, for the energy cut-off of accelerated protons, as many of the underlying parameters are often unknown. Here we analyze experiments on laser proton acceleration in which scans of laser and target parameters were performed. We derive empirical scaling laws from these parameter scans and combine them in a scaling law for the proton energy cut-off that incorporates the laser pulse energy, the laser pulse duration, the focal spot radius, and the target thickness. Using these scaling laws, we give examples for predicting the proton energy cut-off and conversion efficiency for state-of-the-art laser systems.

DOI: 10.1103/PhysRevE.104.045210

I. INTRODUCTION

Since the discovery of laser proton acceleration in the MeV range two decades ago [1], it has attracted great interest due to the prospect of compact laser-based accelerators. Proton and low-Z ion beams are generated by the interaction of high-intensity short pulse lasers with thin foil targets in the micrometer range [2–4]. Laser-accelerated protons have advantageous properties compared to radio-frequency accelerators such as a short pulse duration, high beam densities, and low emittances [5]. With existing petawatt-class lasers, proton acceleration was recently demonstrated up to 94 MeV [6]. This was achieved with laser systems based on neodymium-glass amplifiers, capable of providing high pulse energies, but being limited to typical shot rates of one shot per hour [7–10]. These low repetition rates allow for fundamental research of laser proton acceleration but limit their usefulness for applications. Recently, TW-class laser systems capable of accelerating protons with repetition rates up to 1 kHz have been reported [11–13] as well at PW-class lasers with repetition rates in the range of Hz [14,15]. Laser proton accelerators with such repetition rates would facilitate applications in radio-biology [16,17], fast ignition in inertial confinement fusion [18], and laser-driven neutron sources [19–21]. Each application has different requirements on the produced ion beam energy distribution and the number of ions per pulse. One of the key parameters for laser-accelerated protons is the maximum proton energy—the so-called proton cut-off energy (PCE) E_c. To match the requirements, the laser and target parameters have to be chosen for the desired application.

In this paper, we analyze experimental results on laser ion acceleration from thin foils in the intensity regime of 10^{18} to 10^{22} W/cm^2. For these laser and target parameters, proton and carbon ions are accelerated from the contamination layer at the backside of the foil in a quasistatic electric field, which is created by hot electrons escaping the rear-side target surface. This mechanism is referred to as target normal sheath acceleration (TNSA) [3]. While other acceleration mechanisms have been observed and discussed, the dominant contribution for proton acceleration in this parameter regime is attributed to TNSA [10].

Several analytical models have been proposed to explain proton acceleration in the TNSA regime [43,44]. While the models are typically one-dimensional, they often overestimate the PCE when compared to experiments [22,32], especially at higher intensities. The models also provide scaling laws of the PCE as a function of the intensity $I_0 \simeq E_L/(\tau_L A)$, where E_L is the laser pulse energy, τ_L is the pulse duration, and A is the focal spot area. Laser plasma simulations using the particle-in-cell (PIC) method have been performed in one, two, and three dimensions for predicting proton energies [3]. Most modeling and scaling laws have been discussed on the basis of 1D and 2D simulations [3,45]. 3D PIC simulations

*mzimmer@ikp.tu-darmstadt.de

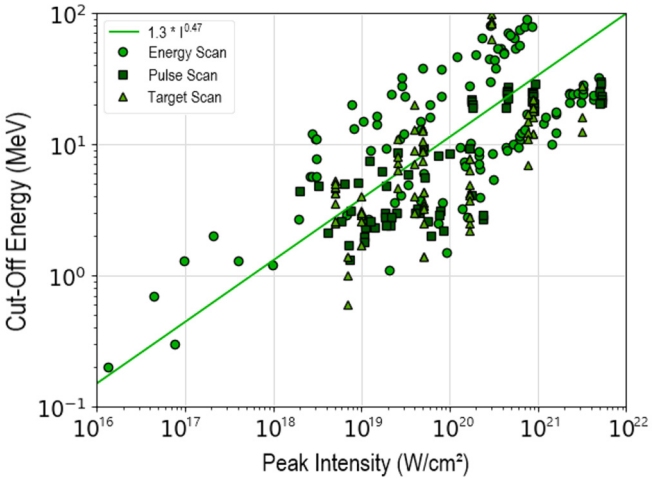

FIG. 1. Proton cut-off energies as a function of peak laser intensity from several experimental data sets [6,22–42]. The linear fit to the experimental data (green line) reveals an average increase in $E_c \propto I_0^{0.47}$. However, deviations from this fit are more than ±400% suggesting that the peak intensity cannot be used as the only parameter for laser proton acceleration.

require extremely large computing resources, in particular when they are performed with high temporal and spatial resolution in order to properly resolve the high plasma frequency of solid density plasmas [46,47]. Therefore, extensive parametric studies using 3D PIC simulations have not been conducted so far for deriving scaling laws of laser ion acceleration. Recently, simulations have been performed in 2D and 3D that can be incorporated in the modeling of TNSA [48]. Generally, 2D simulations overestimate the PCE in comparison to 3D simulations. A recent study has found that the ratio of the PCE from 2D and 3D simulations in the range of 10^{19}–10^{21} W/cm^2 is about a factor of 2 [49]. Another problem for a quantitative comparison of PIC simulations and theoretical models with experiments is that experimental parameters are not known precisely because they are difficult to measure. This can be the front and rear-side plasma scale lengths of the preexpanded foil target which affects the absorption of laser energy into kinetic energy of electrons [50] and thus the magnitude of the TNSA sheath field. Another important parameter is the maximum plasma density, which can be strongly reduced by preexpanded targets, so that other acceleration mechanisms than TNSA can occur in a near-critical density regime. The experimental results can therefore vary between different laser systems and even from shot to shot.

A long-lasting debate has been initiated on how the PCE scales with the intensity of the driving laser [32,51]. A commonly used scaling law predicts a scaling of the proton cut-off energy $E_c \propto \sqrt{I_0}$ [22,52,53]. It has been concluded, for example, by Fuchs *et al.* [22], that this scaling produces acceptable results when changes in intensity are compared at the same laser system and when these changes are caused by a scan of the laser energy. The picture becomes more complicated when the experimental data from different laser facilities are compared. In Fig. 1 we show 274 reported PCEs as a function of the peak laser intensity that was estimated in the respective experiment. The data are collected from 22 publications [6,22–42]. The markers in the plot indicate if the intensity was varied by a scan of the pulse energy or the pulse duration or if a foil thickness scan was performed. In Fig. 8 in the Supplemental Material [54], each data point can be linked to the respective publication by a different color and marker. For the evaluation of this relation, PIC simulations were deliberately excluded to prevent a bias from physical effects that might not appear in the simulation but potentially in the experiments due to unknown exact conditions. From Fig. 1, it is evident that the intensity is not the only parameter that determines the PCE. While the PCE seems to have an overall scaling with $\approx\sqrt{I_0}$, the maximum deviation from this scaling is greater than 400%. The standard deviation for the entire data set to the green fit curve is $\sigma = 123\%$. Accordingly, it is not possible to make an accurate prediction for E_c relying on the intensity as the only variable.

Here we report an analysis of laser proton acceleration experiments that have been published in 22 peer-reviewed articles and compare the data set to find scaling laws in the TNSA regime as a dependency of the laser and target parameters. We investigate in which range of pulse lengths, energies, focal spot sizes, and target thicknesses a consistent power-law scaling can be observed with the experimental data. Based on the published experimental data, we derive an empirical scaling law for the PCE. This approach derives its predictive capability from empirical observations. The exact plasma conditions such as the plasma scale length or the maximum density are neglected to keep the empirical model as simple as possible.

We test the empirical model for the laser system DRACO at the Helmholtz Centre Dresden Rossendorf [55] and make a prediction for upcoming laser proton acceleration experiments at the 10 petawatt HPLS laser at ELI-NP [56].

II. DERIVATION OF INDIVIDUAL SCALING DEPENDENCIES FOR INDIVIDUAL LASER-TARGET PARAMETERS

Laser ion acceleration in the TNSA regime has been investigated by experiments, simulations, and analytical models by several groups [2,3]. A review of the theory of TNSA can be found in Ref. [44]. In this section, we briefly introduce the physical concepts of existing theoretical quantitative scaling models and discuss their problems. In TNSA, a high-power laser pulse is focused on a thin foil with micrometer thickness to intensities above 10^{18} W/cm^2. The solid target is ionized by prepulses or the rising edge of the pulse and the laser field interacts with electrons at the front side plasma density gradient. The laser field is typically given by the amplitude of the normalized vector potential

$$a_0 = \frac{eE_0}{\omega_L m_e c} = \sqrt{\frac{I_0\,[\mathrm{W/cm^2}]\,\lambda^2\,[\mu m]}{1.37\times10^{18}\ \mathrm{W/cm^2/\mu m}}}, \qquad (1)$$

where e is the elementary charge, E_0 is the electric field amplitude, m_e is the electron mass, ω_L is the laser frequency, c is the speed of light, I_0 is the maximum laser intensity in units of W/cm^2, and λ is the central laser wavelength in units of μm. With the normalized vector potential a_0, the ponderomotive

potential of the laser field can be estimated by

$$U_p = m_e c^2\left(\sqrt{1+a_0^2}-1\right), \tag{2}$$

which can be used to estimate the hot electron temperature of the solid density plasma at the surface [57]. The hot electrons propagate through the target and escape at the rear side of the foil. Most theoretical models and simulations assume a step-like plasma profile at the backside, which leads to a strong electric sheath field that accelerates the protons in the contamination layer. In the experiments, however, prepulses can lead to an expansion of the target and the formation of a rear-side plasma density gradient, which reduces the sheath field and the maximum proton energy [58]. To prevent a rear-side plasma density gradient, techniques to provide ultrahigh temporal contrast have been developed [41]. Mora has used the ponderomotive scaling, Eq. (2), to model the expansion of the ions in the sheath field [52]. In the model by Mora, a maximum proton energy

$$E_c = 2m_e c^2\left(\sqrt{1+a_0^2}-1\right)\left[\ln\left(\tau_p+\sqrt{\tau_p^2+1}\right)\right]^2 \tag{3}$$

is predicted with the dimensionless parameter $\tau_p = \omega_{pi}\tau_{\mathrm{acc}}/2.33$. Here ω_{pi} is the plasma ion frequency and τ_{acc} is the acceleration time, which was initially set to be the laser pulse length τ_L. Fuchs *et al.* [22] later modified the acceleration time to $1.3\tau_L$. The scaling law was introduced in 2006 and was widely applied for the interpretation of experiments using laser intensities in the range of 10^{18} to 10^{19} W/cm^2, but overestimates PCEs for higher intensities as discussed in the Supplemental Material [54]. Other models developed by Schreiber and Zeil [33,51,59] produce more accurate results, but rely on assumptions on the hot electron conversion efficiency η_e. While the conversion efficiency can be estimated with $\eta_e = 1.2\times10^{-15}I_0^{3/4}$ [51,60,61], it is known that η_e also depends on other parameters like the target thickness [39,62] or the pulse duration [26]. Consequently, the complex interplay of many factors makes it difficult to predict accurate PCEs without measuring the exact plasma parameters at a given system. This motivates our approach to find an empirical model for the PCE as a function of the main laser and target parameters, the laser energy E_l, the pulse duration τ_L, the focal spot radius r_s and the target thickness d_T. It is known that the polarization and the angle of incidence also have an influence on the absorption [63] and thus the PCE. Most experimental scans have been performed in 45° incidence and *p*-polarization as the absorption by resonance absorption or Brunel heating [64] is high and thus also the PCE. For experiments with normal or close to normal incidence, similar PCEs have been measured in comparison to 45° *p*-polarization which can be explained by a higher projected intensity on the target foil [23]. We can therefore neglect the influence of the incidence angle when small incident angles or *p*-polarization up to 45° is used. For other cases not enough experimental angle and polarization scans have been performed to deduce a reliable scaling law.

A. Influence of peak intensity on proton cut-off energy

We now investigate the dependence of the PCE on the laser intensity in more detail. In Fig. 2 the intensity dependence

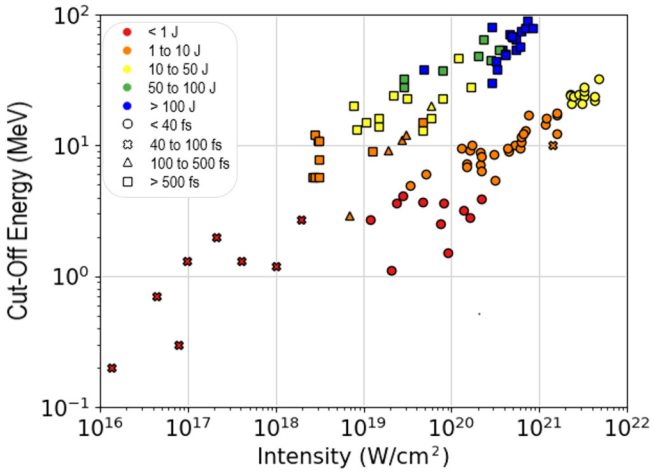

FIG. 2. Proton cut-off energy from 13 experiments [22–34], in which an energy scan has been performed. The highest PCEs were measured using laser systems with high pulse energies > 100 J. Laser systems with lower pulse energies and shorter pulse duration can reach similar intensities, but the observed PCEs were significantly lower.

of the PCE is displayed for experimental data, in which the intensity is varied by the laser pulse energy. Different colors indicate the laser energy for each data point. The marker shape shows the range of the laser pulse duration used. Uncertainties for most experimental data points are below 10% and are lower than the shot-to-shot fluctuations. Error bars are thus not shown in the graph to increase visibility. We can now ask which intensity is required to obtain a certain PCE. In the range between 1 and 30 MeV, the same PCE can be reached by intensities that are two to three orders of magnitude apart. In a similar way, it is possible to ask which PCE can be obtained for a given intensity. Here the data show that the PCE can vary up to one order of magnitude in the regime between 10^{19} and 10^{21} W/cm^2. As an example, for a peak intensity of 2×10^{20} W/cm^2, PCEs between 3 and 68 MeV have been reported. This large variance indicates, as discussed above, that the intensity as a parameter is not sufficient to predict PCEs. However, Fig. 2 shows two clusters that indicate similar intensity scalings. One cluster corresponds to lasers with pulse durations > 500 fs and relatively high pulse energies (square markers). The other cluster is the data set from laser pulses with pulse durations < 40 fs and relatively low pulse energies (circular markers).

B. Influence of laser pulse energy on proton cut-off energy

The analysis of Fig. 2 suggests that the scaling laws must be adapted for different pulse durations and pulse energies. At first, the PCEs are plotted as a function of the laser pulse energy in Fig. 3. The color and shape of the markers indicate again the laser energy and the pulse duration, respectively.

It is evident that this plot shows a drastically decreased spread of the PCE in comparison to Figs. 1 and 2. The standard deviation of E_c below 2 J is reduced to 41% with respect to the fit function of $E_c = 5.3E_L^{0.89}$. Above 2 J the data are described by a fit in the form of $E_c = 7.3E_L^{0.4}$ with a standard deviation of 30%.

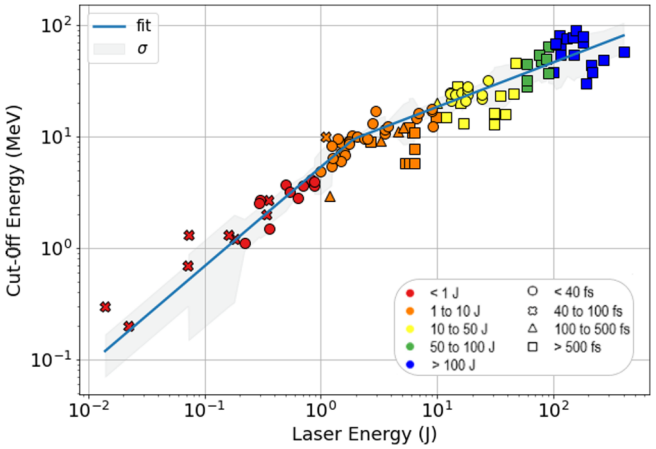

FIG. 3. Proton cut-off energies as a function of laser energy. The data points show a significant decrease in their spread in comparison to Fig. 2. The gray area shows the standard deviation from the fit function $E_c = 5.3E_L^{0.89}$ below 2 J and $E_c = 7.3E_L^{0.4}$ above. The corresponding publications from which the data were extracted can be found in Fig. 7 in the Supplemental Material [54].

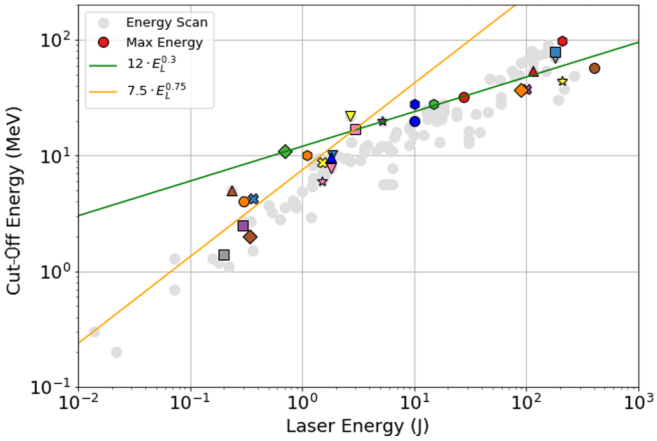

FIG. 4. Proton cut-off energies as a function of laser energy using the same data as Fig. 3. Only the shots with the highest PCE for each scan are highlighted representing the maximum performance of the laser system in terms of laser ion acceleration. These data are fitted to find a function to predict the maximum ion energy of a laser system according to their energy. Below 2 J of laser energy, the cut-off energy scales with $E_c = 7.5I^{0.75}$ and for higher energies it follows $E_c = 12I^{0.3}$. The data points were taken from [6,22–42].

This is a significantly reduced spread compared to the 123% variation for the intensity dependence in Fig. 1. This means that the pulse energy can describe the empirical data much better than the intensity.

The peak intensity is calculated using Gaussian optics to

$$I_0 = q\frac{E_L}{\tau_L A} = q'\frac{E_L}{\tau_L \frac{\pi r_s^2}{\ln(2)}}. \tag{4}$$

The quality factor q takes effects into account that reduce the intensity such as wavefront errors or non-Gaussian pulse shapes. We have taken the q value from the publication or have set it to 1 in the analysis if not specified in the respective publication. Interestingly, the graph in Fig. 3 shows a change in the slope at around 2 J, which appears to be independent of the pulse length and intensity. Why this change in scaling occurs at 2 J requires further investigation.

Figure 3 shows that the laser energy serves as a more accurate indicator for the PCE than the laser intensity. In the following section, we aim at quantifying the influence of the laser energy on the PCE by finding a scaling law. Most data sets that previously investigated this dependence conducted an energy scan that simultaneously increased the intensity as well. This is problematic as it is known that an increase in intensity at constant E_L is capable of affecting the PCE [26]. Therefore, it cannot be ruled out that the increase in PCE is partly caused by the higher intensity, more precisely the higher electromagnetic fields, instead of the larger amount of energy deposited into the interaction region. To find the influence of the latter, one ideally would need a data set where the energy is varied but the intensity is kept constant. Such a data set with a sufficient amount of shots has not been published to our knowledge. We therefore include only one data point per scan, thus aiming for a statistical variance of the other parameters that determine the intensity, i.e., the pulse duration and the focal spot size to average out the influence of I_0. We selected the data points with the highest E_L, smallest d_T or shortest τ_L published in each scan, shown in Fig, 1.

This subset of data points is displayed in Fig. 4 and has a Pearson correlation coefficient between the laser pulse energy and the peak intensity of -0.004. With a correlation at this low level, it can be seen as justified to assume that changes in the PCE are caused only by changes in the laser energy using the described procedure. In Fig. 4 we observe again that the scaling with the laser energy exhibits a change at around 2 J. For this reason, the empirical scaling law is divided into two regions. Below 2 J, the PCE scaling with E_L is described by the function $E_c = 7.5E_L^{0.75}$ and for higher energies the PCE can be described by $E_c = 12E_L^{0.3}$. The standard deviation of the fitting curve for lower pulse energies is 45% and 24% for higher energies. Further investigations of existing data sets have shown that the laser energy additionally influences the conversion efficiency with a linear dependency up to around 10%; see the Supplemental Material [54] including Refs. [1,6,10,22,24,29,31,31,32,38,39,42,65–70].

C. Influence of laser pulse duration on proton cut-off energy

We now investigate the influence of the pulse duration τ_L on the PCE. In Fig. 5 seven data sets of pulse duration scans are displayed. The experimental PCEs [30] are shown as a function of intensity, while changes in intensity were caused by variations in pulse length. All other parameters were held constant. The PCE scaling is fitted to a function

$$E_c(I) = AI_0^b. \tag{5}$$

Including all seven data sets, a mean value for $b = 0.09(8)$ has been found, which is a drastic deviation from the intensity dependence that is given by the scaling laws, e.g., $E_c \propto \sqrt{I_0} \propto a_0$ and contradicts existing theories [22]. This effect is attributed to a balance between competing counteracting processes for an effective acceleration. A decrease in intensity causes a lower laser ponderomotive potential [22,71], leading to a drop in electron temperature. Longer pulses, on

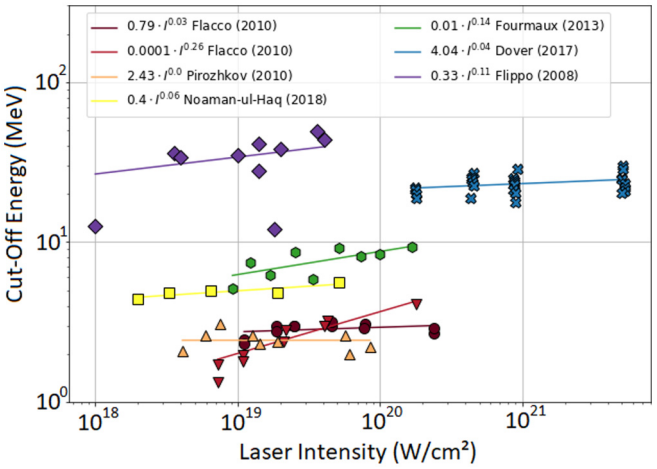

FIG. 5. Comparison of pulse length scans from six experiments [26,29,30,34–36]. The shape of the marker groups the data sets. The color represents the laser energy whereby blue corresponds to the highest and red to the lowest pulse energy. The fits characterize the dependency of the PCEs on the intensity caused by changes in the pulse length using $E_c(I) = AI^b$.

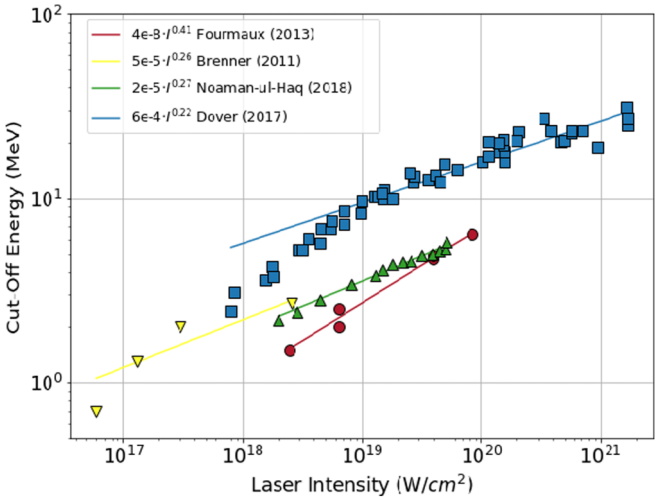

FIG. 6. Proton cut-off energies (PCEs) as a function of the intensity that has been varied experimentally by a focal spot size scan. Four experiments are included in the analysis [26,27,30,34]. Fits of the intensity scaling were performed, leading to an average scaling of $E_c \propto I^{0.29(7)}$.

the other hand, have shown to reduce the reflectivity on the target surface [26], which increases the conversion efficiency. In addition, electrons are able to recirculate more often in longer pulses, which increases the electron temperature. For short pulses, especially below 100 fs, the acceleration time is limited through the shorter pulse duration. This can also lead to a reduction of the cut-off energies. The observation of a weak dependence on the pulse length is reinforced by the data from Fig. 2 as the PCE displays only a weak dependence on the intensity while most changes can be attributed to a higher laser energy, as indicated by the color coding. In future experiments, it has to be investigated how this effect changes at pulse lengths above 1 ps.

D. Influence of focal spot size on proton cut-off energy

The next parameter that has to be investigated in detail is the focal spot size. In an ideal case, a parameter scan would be conducted using focusing mirrors with different F-numbers and therefore different focal spot radii. This is, however, impractical and a spot size scan is typically performed by changing the position of the target foil relative to the focal point. Then the spot radius becomes larger, but the spot profile typically deviates from a Gaussian profile for nonideal beam shapes. Changes in intensity were used to calculate an effective focal spot size r_s according to Eq. (4).

Similar to the procedure for the pulse duration, we analyze several intensity scans that have been performed by changing the focal spot size. In Fig. 6 four data sets are displayed, which reveal a PCE dependence of the intensity via a focal spot-size scan. An average scaling law $E_c \propto I_0^{0.29(7)}$ has been found, which translates to $E_c \propto r_s^{-0.58(16)}$ for the spot radius r_s. It is worth noting that the energy scaling combined with the scaling caused by the focal scan results in a scaling with $E_c \propto E_L^{0.30(3)} I_0^{0.29(8)} \equiv I_0^{0.59(9)}$. This exponent is close to the $\sqrt{I_0}$-scaling observed when both values are increased at the same time. This further strengthens the hypothesis that the PCE shows different scaling rates depending on which parameter is changed to increase the intensity. This implies that an increase in laser energy that causes an increase in intensity scales the PCE with $E_L^{0.59(9)}$. In contrast to that, an increase in laser energy at constant intensity is expected to scale the PCE with $\propto E_L^{0.30(3)}$.

E. Influence of target thickness on proton cut-off energy

The target plays a significant role in laser ion acceleration experiments. The PCE has been increased significantly using micro- and nanostructured targets [65,72] or ultrathin targets [38,41]. Here we concentrate on experiments using thin flat foil targets, that have been used as standard targets at many laboratories. We also do not differentiate between target materials and target roughness, even though this has been proven to influence preplasma formation, absorption and thus also the PCEs [3,73]. The foil thickness d_T is the only parameter that we investigate for deriving an empirical scaling law. Target thickness scans have been performed by many groups [39,40,58,74]. The experiments have shown that the PCEs increases for thinner targets [41] until a minimum target thickness $d_{\min}$ is reached. This minimum target thickness depends, among other parameters, on the temporal contrast of the laser pulse [58]. Simulations have shown that prepulses can ionize the target before the arrival of the main pulse and a shock wave reaches the rear side of the target, leading to a rear-side plasma density gradient and a reduced PCE [58]. To find empirical scaling laws from experiments, only data are used where the target thickness was above $d_{\min}$ and the influence of the laser pulse contrast can be neglected. Figure 7 shows 11 thickness scans from published experiments. The marker and the fit line style indicate individual data sets. The color attributes the laser pulse energy that has been used in the experiment. Red colored points and lines signal data

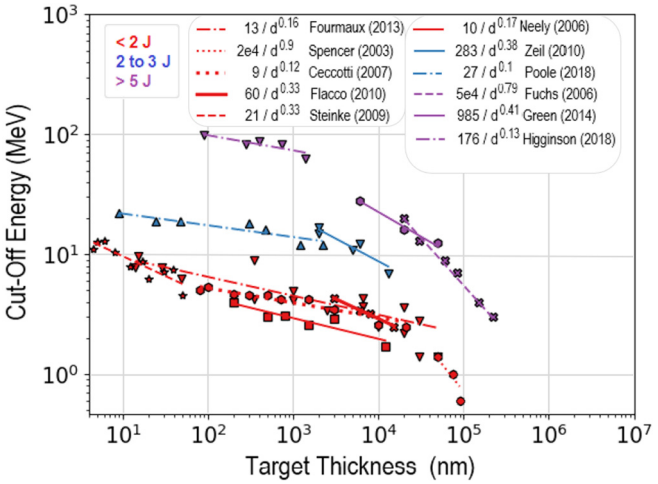

FIG. 7. Proton cut-off energies as a function of the target thickness from various experiments [6,22,26,33,35,37–42]. Only experimental data are included that show an increase of the PCE with decreasing target thickness. Red data points have laser energies below 2 J, blue markers are between 2 and 3 J and purple markers are above 5 J. It can be seen that similar laser energies lead to similar scaling behavior.

sets with $E_L < 2$ J, blue points between 2 and 3 J, and purple markers indicate experiments with > 5 J. Similar to the strategy above, we try to find scaling laws for the PCE as a function of the target thickness. We use a scaling law

$$E_c \propto d_T^b, \tag{6}$$

where b is the exponent that is fitted using the experimental data. The red data sets, which were obtained with six different laser systems, show a very similar behavior, where three thickness regimes are visible. The first regime is between 10 and 100 μm, in which the PCE scales rapidly with $d_T^{-0.7(2)}$. In this range, d_T is much larger than r_s and electrons spread spatially over a larger area, reducing the sheath strength for thicker targets [58]. The second regime between 10 μm and 100 nm shows a lower median scaling with $\propto d_T^{-0.16(10)}$. In this range, the electron spread becomes negligible, and for thinner targets the electrons lose less energy while propagating through the target and can recirculate more efficiently [39,69]. For targets below 100 nm, two data sets show an increase in the scaling rate $\propto d_T^{-0.33(8)}$. This strong increase in the PCE for very thin foil targets is consistent with the onset of relativistic transparency [40,75]. A similarly strong dependency was found for the conversion efficiency with target thickness with $\propto d^{-0.49(25)}$, further discussed in the Supplemental Material [54], including Refs. [6,22,38,39,42].

III. DEVELOPMENT OF AN EMPIRICAL SCALING FOR LASER PROTON ACCELERATION

The results for the empirical scalings of the PCE for the laser pulse energy, the laser pulse duration, the spot radius and the target thickness are summarized in Table I. These scalings

TABLE I. Summary of the scaling parameters for the proton cut-off energy. We assume that the PCE is proportional to a parameter X^b with an exponent b that is empirically determined by a fit to a large experimental data set.

Laser or target parameter	Scaling exponent b
E_L	0.30(3)
τ_L	−0.09(8)
r_s	−0.58(16)
d_T	−0.16(10)

can be combined into one equation

$$E_c^* = E_c^r \cdot \left(\frac{E_L^*}{E_L^r}\right)^{0.59} \left(\frac{\tau_L^*}{\tau_L^r}\right)^{-0.09} \left(\frac{r_s^*}{r_s^r}\right)^{-0.58} \left(\frac{d_T^*}{d_T^r}\right)^{-0.16}, \tag{7}$$

which allows an estimate of the PCE, E_c^* for given laser and target parameters $(E_L^*, \tau_L^*, r_s^*, d_T^*)$. For this estimate, one has to choose a reference data point $(E_c^r, E_L^r, \tau_L^r, r_s^r, d_T^r)$ from an experiment, which is closest in the four-dimensional parameter space. While it is not always clear, which reference data point to use, it is beneficial to repeat the estimate with three or more data points and calculate an average to minimize statistical uncertainties. We test this procedure for the 150-TW laser system DRACO at the Helmholtz Centre Dresden Rossendorf ($E_L^* = 2.7$ J, $\tau_L^* = 30$ fs, $r_s^* = 1.5$ μm, $d_T^* = 2$ μm). As references, we use the experimental data from Astra Gemini (Rutherford Appleton Laboratory) [42], J-KAREN-P (Osaka) [34], and ALLS (INRS-EMT) [26]. The results are shown in Table II. The spread of the projected PCE, E_c^* is quite large (16 MeV, 10 MeV, 7 MeV). However, the average E_c^* is 11(4) MeV which is very close to the reported value of 12 MeV [40].

We now want to use this procedure to extrapolate the PCE for recently developed laser systems. The 10 petawatt HPLS laser at the Extreme Light Infrastructure–Nuclear Physics (ELI-NP) has been inaugurated in November 2020 demonstrating 200 J in 20 fs [15]. As reference data, we use experimental data from the PHELIX laser at the GSI Darmstadt [23], the Vulcan laser at RAL [6], the Titan laser at LLNL [76], J-KAREN-P at Osaka University [34], and the DRACO laser at HZDR [40,77]. The laser and target parameters of the reference data can be seen in Table III. The predicted PCEs for ELI-NP range from 120 to 164 MeV.

TABLE II. Prediction of the PCE of the DRACO laser based on the proposed scaling model. The projected cut-off energy E_c^* for the DRACO laser is calculated with Eq. (7) based on three different experiments [26,34,42] to compare it to the experimental PCE observed by Poole *et al.* [40] for these parameters. The predicted mean value of 11 MeV closely matches the reported 12 MeV in the experiment.

Laser	E_L [J]	τ_L [fs]	r_s [μm]	d_T [μm]	E_c^r [MeV]	E_c^* [MeV]
GEMINI	10	45	1.25	6	28	16
J-KAREN-P	28	30	2	2	32	10
ALLS	1.8	30	2.8	1	4.1	7
DRACO	2.7	30	1.5	1.25	12	11(4)

TABLE III. Projection of the proton cut-off energy of the 10 PW laser system at ELI-NP based on the empirical scaling, Eq. (7). The average predicted cut-off energy for ELI-NP is 145(14) MeV. Data refer to experiments from [6,23,34,40,76,77]

Laser	E_L [J]	τ_L [fs]	r_s [μm]	d_T [μm]	E_c^r [MeV]	E_c^* [MeV]
PHELIX	180	500	1.5	1.5	79	120
VULCAN	210	900	2.9	0.09	98	134
TITAN	180	700	4.5	10	40	160
J-KAREN-P	28	30	2.0	2	32	140
DRACO	2.7	30	1.5	1.25	12	164
DRACO-PW	18	30	1.3	0.4	45	154
ELI-NP	200	20	1.5	1	—	145(14)

This results in an average PCE of $E_c^* = 145(14)$ MeV, predicted by this empirical scaling model with these reference data. This projection of the PCE is significantly lower that estimated by the Fuchs scaling [22] (1.0 GeV), the Zeil scaling [33] (745 MeV), or the relativistic Schreiber model [51] (844 MeV) and will be tested in the following years by experiments on laser proton acceleration at ELI-NP. The empirical scaling [Eq. (7)] has intrinsic limitations. On the one hand, the here developed scaling exploited data with intensities ranging from 10^{16} to 10^{21} W/cm^2, pulse lengths between 30 fs and 1 ps and energies between 10 mJ and 400 J. Novel ion acceleration mechanisms have been predicted at the high-intensity frontier of this parameter space. For example, ion acceleration by radiation pressure has been observed in experiments [78] and simulations [79] using very thin foils. Since it was found in Sec. II E that the scaling with target thickness changes below 100 nm and above 50 μm, predictions in this range should be taken with caution. It should also be noted that the empirical scaling for the target thickness can only be applied when the laser contrast is high enough so that $d > d_{\min}$.

IV. CONCLUSION

In this paper, we analyzed the parametric dependence of laser proton acceleration using numerous experimental data sets. Motivated by theoretical models of the TNSA mechanism, we investigated the proton cut-off energy as a function of the laser intensity. We found, however, that the PCE is not well described by the intensity alone. We therefore investigated the PCE as a function of the laser pulse energy E_L, laser pulse duration τ_L, laser spot radius r_s, and the foil thickness d_T. Empirical scaling laws for the PCE were retrieved for the different parameters using large experimental data sets from peer-reviewed publications with typical laser and target parameters. We found that the PCE depends on the combination of laser pulse energy E_L, the pulse duration τ_L, the focal spot radius r_s, and the target thickness d_T, rather than the peak intensity and follows individual scaling laws for each parameter. Table I summarizes the different scaling dependencies of the PCE for these parameters, that were obtained by fitting the power laws to the experimental data sets. It can be concluded that the focal spot radius has the largest impact on the PCE, followed by E_L and the target thickness. The pulse duration τ_L has the lowest impact between 30 fs and 1 ps. An empirical scaling law was obtained [Eq. (7)], which incorporates E_L, τ_L, r_s, and d_T. This scaling can be used for an estimate of the PCE for a given laser system. For such an estimate, reference data must be included. We tested the empirical scaling law by predicting the PCE for the 150-TW laser system DRACO at the HZDR. The average prediction of 11(4) MeV is close to the reported value of 12 MeV. We further used the empirical scaling for a prediction of the PCE at the 10 PW HPLS laser at ELI-NP. An average PCE of 145(14) MeV was found using six different data points as a reference.

ACKNOWLEDGMENTS

This work is supported by the Hessian Ministry for Science and the Arts (HMWK) through the LOEWE Research Cluster Nuclear Photonics. M.Z. conceived the study, collected and analyzed the data, and developed the scaling laws. C.R., J.H., and V.B. helped to develop the structure of the manuscript. M.Z., C.R., and S.S. wrote the manuscript. T.E., G.S., V.B., and B.S. provided valuable insights on the theoretical foundations. All authors commented on the manuscript.

[1] R. Snavely, M. H. Key, S. P. Hatchett, T. E. Cowan, M. Roth, T. W. Phillips, M. A. Stoyer, E. A. Henry, T. C. Sangster, M. S. Singh *et al.*, Phys. Rev. Lett. **85**, 2945 (2000).

[2] H. Daido, M. Nishiuchi, and A. S. Pirozhkov, Rep. Prog. Phys. **75**, 056401 (2012).

[3] A. Macchi, *Applications of Laser-Driven Particle Acceleration*, edited by P. Bolton, K. Parodi, and J. Schreiber (CRC Press, Boca Raton, 2020).

[4] M. Roth and M. Schollmeier, CERN Yellow Rep. **1**, 231 (2016).

[5] T. E. Cowan, J. Fuchs, H. Ruhl, A. Kemp, P. Audebert, M. Roth, R. Stephens, I. Barton, A. Blazevic, E. Brambrink *et al.*, Phys. Rev. Lett. **92**, 204801 (2004).

[6] A. Higginson, R. Gray, M. King, R. Dance, S. Williamson, N. Butler, R. Wilson, R. Capdessus, C. Armstrong, J. Green *et al.*, Nat. Commun. **9**, 724 (2018).

[7] V. Bagnoud, B. Aurand, A. Blazevic, S. Borneis, C. Bruske, B. Ecker, U. Eisenbarth, J. Fils, A. Frank, E. Gaul *et al.*, Appl. Phys. B **100**, 137 (2010).

[8] M. Martinez, W. Bang, G. Dyer, X. Wang, E. Gaul, T. Borger, M. Ringuette, M. Spinks, H. Quevedo, A. Bernstein *et al.*, in *AIP Conference Proceedings*, Vol. 1507 (American Institute of Physics, Austin, Texas, USA, 2012), pp. 874–878.

[9] J. Schreiber, P. Bolton, and K. Parodi, Rev. Sci. Instrum. **87**, 071101 (2016).

[10] F. Wagner, O. Deppert, C. Brabetz, P. Fiala, A. Kleinschmidt, P. Poth, V. A. Schanz, A. Tebartz, B. Zielbauer, M. Roth *et al.*, Phys. Rev. Lett. **116**, 205002 (2016).

[11] B. Le Garrec, S. Sebban, D. Margarone, M. Precek, S. Weber, O. Klimo, G. Korn, and B. Rus, *Proceedings of SPIE - The International Society for Optical Engineering* (SPIE, USA, 2014).

[12] K. Nakamura, H. Mao, A. J. Gonsalves, H. Vincenti, D. E. Mittelberger, J. Daniels, A. Magana, C. Toth, and W. P. Leemans, IEEE J. Quantum Electron. **53**, 1 (2017).

[13] C. Herkommer, P. Krötz, S. Klingebiel, C. Wandt, D. Bauer, K. Michel, R. Kienberger, and T. Metzger, in *2019 Conference on Lasers and Electro-Optics (CLEO)* (IEEE, San Jose, California, 2019), pp. 1–2.

[14] C. N. Danson, C. Haefner, J. Bromage, T. Butcher, J.-C. F. Chanteloup, E. A. Chowdhury, A. Galvanauskas, L. A. Gizzi, J. Hein, D. I. Hillier *et al.*, High Power Laser Sci. Eng. **7**, e54 (2019).

[15] F. Lureau, G. Matras, O. Chalus, C. Derycke, T. Morbieu, C. Radier, O. Casagrande, S. Laux, S. Ricaud, and G. Rey, High Power Laser Sci. Eng. **8**, e43 (2020).

[16] S. Bulanov, H. Daido, T. Z. Esirkepov, V. Khoroshkov, J. Koga, K. Nishihara, F. Pegoraro, T. Tajima, and M. Yamagiwa, in *AIP Conference Proceedings*, Vol. 740 (American Institute of Physics, Bajina Basta, 2004), pp. 414–429.

[17] E. Bayart, A. Flacco, O. Delmas, L. Pommarel, D. Levy, M. Cavallone, F. Megnin-Chanet, E. Deutsch, and V. Malka, Sci. Rep. **9**, 10132 (2019).

[18] M. Roth, T. E. Cowan, M. H. Key, S. P. Hatchett, C. Brown, W. Fountain, J. Johnson, D. M. Pennington, R. A. Snavely, S. C. Wilks *et al.*, Phys. Rev. Lett. **86**, 436 (2001).

[19] M. Roth, D. Jung, K. Falk, N. Guler, O. Deppert, M. Devlin, A. Favalli, J. Fernandez, D. Gautier, M. Geissel *et al.*, Phys. Rev. Lett. **110**, 044802 (2013).

[20] D. P. Higginson, J. M. McNaney, D. C. Swift, T. Bartal, D. S. Hey, R. Kodama, S. Le Pape, A. Mackinnon, D. Mariscal, H. Nakamura *et al.*, Phys. Plasmas **17**, 100701 (2010).

[21] M. Zimmer, Laser-driven neutron sources—A compact approach to non-destructive material analysis, Ph.D. thesis, Technische Universität Darmstadt, 2020.

[22] J. Fuchs, P. Antici, E. d'Humières, E. Lefebvre, M. Borghesi, E. Brambrink, C. Cecchetti, M. Kaluza, V. Malka, M. Manclossi *et al.*, Nat. Phys. **2**, 48 (2006).

[23] J. Hornung, Y. Zobus, P. Boller, C. Brabetz, U. Eisenbarth, T. Kühl, Z. Major, J. Ohland, M. Zepf, B. Zielbauer *et al.*, High Power Laser Sci. Eng. **8**, e24 (2020).

[24] C. Zulick, F. Dollar, V. Chvykov, J. Davis, G. Kalinchenko, A. Maksimchuk, G. Petrov, A. Raymond, A. Thomas, L. Willingale *et al.*, Appl. Phys. Lett. **102**, 124101 (2013).

[25] Y. Fang, X. Ge, S. Yang, W. Wei, T. Yu, F. Liu, M. Chen, J. Liu, X. Yuan, Z. Sheng *et al.*, Plasma Phys. Control. Fusion **58**, 075010 (2016).

[26] S. Fourmaux, S. Buffechoux, B. Albertazzi, D. Capelli, A. Lévy, S. Gnedyuk, L. Lecherbourg, P. Lassonde, S. Payeur, P. Antici *et al.*, Phys. Plasmas **20**, 013110 (2013).

[27] C. Brenner, J. Green, A. Robinson, D. Carroll, B. Dromey, P. Foster, S. Kar, Y. Li, K. Markey, C. Spindloe *et al.*, Laser Part. Beams **29**, 345 (2011).

[28] S. Busold, Construction and characterization of a laser-driven proton beamline at GSI, Ph.D. thesis, Technische Universität Darmstadt, 2014.

[29] K. Flippo, J. Workman, D. Gautier, S. Letzring, R. Johnson, and T. Shimada, Rev. Sci. Instrum. **79**, 10E534 (2008).

[30] M. Noaman-ul Haq, H. Ahmed, T. Sokollik, Y. Fang, X. Ge, X. Yuan, and L. Chen, Nucl. Instrum. Methods Phys. Res. A **909**, 164 (2018).

[31] M. Zepf, E. Clark, K. Krushelnick, F. Beg, C. Escoda, A. Dangor, M. Santala, M. Tatarakis, I. Watts, P. Norreys *et al.*, Phys. Plasmas **8**, 2323 (2001).

[32] L. Robson, P. Simpson, R. J. Clarke, K. W. Ledingham, F. Lindau, O. Lundh, T. McCanny, P. Mora, D. Neely, C.-G. Wahlström *et al.*, Nat. Phys. **3**, 58 (2007).

[33] K. Zeil, S. Kraft, S. Bock, M. Bussmann, T. Cowan, T. Kluge, J. Metzkes, T. Richter, R. Sauerbrey, and U. Schramm, New J. Phys. **12**, 045015 (2010).

[34] N. Dover, https://agenda.infn.it/event/12611/contributions/15387/attachments/11296/12698/WG2_summary.pdf (2017).

[35] A. Flacco, F. Sylla, M. Veltcheva, M. Carrié, R. Nuter, E. Lefebvre, D. Batani, and V. Malka, Phys. Rev. E **81**, 036405 (2010).

[36] A. S. Pirozhkov, H. Daido, M. Nishiuchi, and K. Ogura, in *Advances in Solid State Lasers Development and Applications*, edited by M. Grishin (IntechOpen, 2010), pp. 609–630.

[37] I. Spencer, K. W. D. Ledingham, P. McKenna, T. McCanny, R. P. Singhal, P. Foster, D. Neely, A. J. Langley, E. J. Divall, C. J. Hooker *et al.*, Phys. Rev. E **67**, 046402 (2003).

[38] S. Steinke, A. Henig, M. Schnürer, T. Sokollik, P. Nickles, D. Jung, D. Kiefer, R. Hörlein, J. Schreiber, T. Tajima *et al.*, Laser and Particle Beams **28**, 215 (2010).

[39] D. Neely, P. Foster, A. Robinson, F. Lindau, O. Lundh, A. Persson, C.-G. Wahlström, and P. McKenna, Appl. Phys. Lett. **89**, 021502 (2006).

[40] P. Poole, L. Obst, G. Cochran, J. Metzkes, H. Schlenvoigt, I. Prencipe, T. Kluge, T. Cowan, U. Schramm, D. Schumacher *et al.*, New J. Phys. **20**, 013019 (2018).

[41] T. Ceccotti, A. Lévy, H. Popescu, F. Réau, P. d'Oliveira, P. Monot, J. P. Geindre, E. Lefebvre, and P. Martin, Phys. Rev. Lett. **99**, 185002 (2007).

[42] J. Green, A. Robinson, N. Booth, D. Carroll, R. Dance, R. Gray, D. MacLellan, P. McKenna, C. Murphy, D. Rusby *et al.*, Appl. Phys. Lett. **104**, 214101 (2014).

[43] M. Passoni and M. Lontano, Phys. Rev. Lett. **101**, 115001 (2008).

[44] M. Passoni, L. Bertagna, and A. Zani, New J. Phys. **12**, 045012 (2010).

[45] T. Esirkepov, M. Yamagiwa, and T. Tajima, Phys. Rev. Lett. **96**, 105001 (2006).

[46] A. Sharma and A. Andreev, Laser Part. Beams **34**, 219 (2016).

[47] S. Göde, C. Rödel, K. Zeil, R. Mishra, M. Gauthier, F.-E. Brack, T. Kluge, M. J. MacDonald, J. Metzkes, L. Obst *et al.*, Phys. Rev. Lett. **118**, 194801 (2017).

[48] J. Babaei, L. A. Gizzi, P. Londrillo, S. Mirzanejad, T. Rovelli, S. Sinigardi, and G. Turchetti, Phys. Plasmas **24**, 043106 (2017).

[49] K. D. Xiao, C. T. Zhou, K. Jiang, Y. C. Yang, R. Li, H. Zhang, B. Qiao, T. W. Huang, J. M. Cao, T. X. Cai, M. Y. Yu *et al.*, Phys. Plasmas **25**, 023103 (2018).

[50] S. Bastiani, A. Rousse, J. P. Geindre, P. Audebert, C. Quoix, G. Hamoniaux, A. Antonetti, and J. C. Gauthier, Phys. Rev. E **56**, 7179 (1997).

[51] J. Schreiber, F. Bell, and Z. Najmudin, High Power Laser Sci. Eng. **2**, e41 (2014).

[52] P. Mora, Phys. Rev. E **72**, 056401 (2005).

[53] L. Torrisi, Nukleonika **60**, 207 (2015).

[54] See Supplemental Material at http://link.aps.org/supplemental/10.1103/PhysRevE.104.045210 for comparison of existing scaling laws with experimental data for cutt-off energies and laser ion conversion efficiency.
[55] U. Schramm, M. Bussmann, A. Irman, M. Siebold, K. Zeil, D. Albach, C. Bernert, S. Bock, F. Brack, J. Branco *et al.*, J. Phys.: Conf. Ser. **874**, 012028 (2017).
[56] K. Tanaka, K. Spohr, D. Balabanski, S. Balascuta, L. Capponi, M. Cernaianu, M. Cuciuc, A. Cucoanes, I. Dancus, A. Dhal *et al.*, Matter Radiat. Extremes **5**, 024402 (2020).
[57] S. C. Wilks, W. L. Kruer, M. Tabak, and A. B. Langdon, Phys. Rev. Lett. **69**, 1383 (1992).
[58] M. Kaluza, J. Schreiber, M. I. Santala, G. D. Tsakiris, K. Eidmann, J. Meyer-ter Vehn, and K. J. Witte, Phys. Rev. Lett. **93**, 045003 (2004).
[59] J. Schreiber, F. Bell, F. Grüner, U. Schramm, M. Geissler, M. Schnürer, S. Ter-Avetisyan, B. M. Hegelich, J. Cobble, E. Brambrink *et al.*, Phys. Rev. Lett. **97**, 045005 (2006).
[60] J. Yu, Z. Jiang, J. Kieffer, and A. Krol, Phys. Plasmas **6**, 1318 (1999).
[61] M. Key, M. Cable, T. Cowan, K. Estabrook, B. Hammel, S. Hatchett, E. Henry, D. Hinkel, J. Kilkenny, J. Koch *et al.*, Phys. Plasmas **5**, 1966 (1998).
[62] F. Beg, A. Thomas, and K. Krushelnick, State-of-the-art high flux mono-energetic ion sources driven by ultra-intense laser pulses, Technical Report OMB No. 0704-0188, University of California, San Diego (2019).
[63] M. Cerchez, R. Jung, J. Osterholz, T. Toncian, O. Willi, P. Mulser, and H. Ruhl, Phys. Rev. Lett. **100**, 245001 (2008).
[64] P. Gibbon, in *Proceedings of the 2014 CAS-CERN Accelerator School: Plasma Wake Acceleration*, edited by Edited by B. Holzer (CERN, Geneva, 2016).
[65] S. Gaillard, T. Kluge, K. Flippo, M. Bussmann, B. Gall, T. Lockard, M. Geissel, D. Offermann, M. Schollmeier, Y. Sentoku *et al.*, Phys. Plasmas **18**, 056710 (2011).
[66] C. M. Brenner, A. Robinson, K. Markey, R. Scott, R. Gray, M. Rosinski, O. Deppert, J. Badziak, D. Batani, J. Davies *et al.*, Appl. Phys. Lett. **104**, 081123 (2014).
[67] M. Allen, Y. Sentoku, P. Audebert, A. Blazevic, T. Cowan, J. Fuchs, J. Gauthier, M. Geissel, M. Hegelich, S. Karsch *et al.*, Phys. Plasmas **10**, 3283 (2003).
[68] P. McKenna, K. Ledingham, S. Shimizu, J. Yang, L. Robson, T. McCanny, J. Galy, J. Magill, R. Clarke, D. Neely *et al.*, Phys. Rev. Lett. **94**, 084801 (2005).
[69] A. Mackinnon, Y. Sentoku, P. Patel, D. Price, S. Hatchett, M. Key, C. Andersen, R. Snavely, and R. Freeman, Phys. Rev. Lett. **88**, 215006 (2002).
[70] P. McKenna, D. Carroll, O. Lundh, F. Nürnberg, K. Markey, S. Bandyopadhyay, D. Batani, R. Evans, R. Jafer, S. Kar *et al.*, Laser Part. Beams **26**, 591 (2008).
[71] P. Mora, Phys. Rev. Lett. **90**, 185002 (2003).
[72] D. Margarone, O. Klimo, I. Kim, J. Prokupek, J. Limpouch, T. Jeong, T. Mocek, J. Psikal, H. Kim, J. Proska *et al.*, Phys. Rev. Lett. **109**, 234801 (2012).
[73] T. Ebert, N. W. Neumann, L. N. Döhl, J. Jarrett, C. Baird, R. Heathcote, M. Hesse, A. Hughes, P. McKenna, D. Neely *et al.*, Phys. Plasmas **27**, 043106 (2020).
[74] D. Batani, R. Jafer, M. Veltcheva, R. Dezulian, O. Lundh, F. Lindau, A. Persson, K. Osvay, C. Wahlström, D. Carroll *et al.*, New J. Phys. **12**, 045018 (2010).
[75] V. Bagnoud, J. Hornung, T. Schlegel, B. Zielbauer, C. Brabetz, M. Roth, P. Hilz, M. Haug, J. Schreiber, and F. Wagner, Phys. Rev. Lett. **118**, 255003 (2017).
[76] M. Barberio, M. Scisciò, S. Vallières, F. Cardelli, S. Chen, G. Famulari, T. Gangolf, G. Revet, A. Schiavi, M. Senzacqua *et al.*, Nat. Commun. **9**, 372 (2018).
[77] T. Ziegler, D. Albach, and K. Zeil, Sci Rep **11**, 7338 (2021).
[78] S. Kar, K. F. Kakolee, B. Qiao, A. Macchi, M. Cerchez, D. Doria, M. Geissler, P. McKenna, D. Neely, J. Osterholz *et al.*, Phys. Rev. Lett. **109**, 185006 (2012).
[79] A. P. L. Robinson, M. Zepf, S. Kar, R. G. Evans, and C. Bellei, New J. Phys. **10**, 013021 (2008).

Correction: The author order was presented incorrectly and has been fixed, necessitating a change to the style in which the affiliations are presented.